Langmuir

Article

pubs.acs.org/Langmuir

Improving the Dielectric Properties of Ethylene-Glycol Alkanethiol Self-Assembled Monolayers

Irene Zaccari,[†] Benjamin G. Catchpole,[†] Sophie X. Laurenson,[‡] A. Giles Davies,[†] and Christoph Wälti*[,†]

[†]University of Leeds, School of Electronic and Electrical Engineering, Woodhouse Lane, Leeds LS2 9JT, United Kingdom

[‡]Abbott GmbH & Co, Max Planck Ring 2, 65205 Wiesbaden, Germany

Supporting Information

ABSTRACT: Self-assembled monolayers (SAMs) can be formed at the interface between solids and fluids, and are often used to modify the surface properties of the solid. One of the most widely employed SAM systems is exploiting thiol-gold chemistry, which, together with alkane-chain-based molecules, provides a reliable way of SAM formation to modify the surface properties of electrodes. Oligo ethylene-glycol (OEG) terminated alkanethiol monolayers have shown excellent antifouling properties and have been used extensively for the coating of biosensor electrodes to minimize nonspecific binding. Here, we report the investigation of the dielectric properties of COOH-capped OEG monolayers and demonstrate a strategy to improve the dielectric properties significantly by mixing the OEG SAM with small concentrations of 11-mercaptoundecanol (MUD). The monolayer properties and composition were characterized by means of impedance spectroscopy, water contact angle, ellipsometry and X-ray photoelectron spectroscopy. An equivalent circuit model is proposed to interpret the EIS data and to determine the conductivity of the monolayer. We find that for increasing MUD concentrations up to about 5% the resistivity of the SAM steadily increases, which together with a considerable decrease of the phase of the impedance, demonstrates significantly improved dielectric properties of the monolayer. Such monolayers will find widespread use in applications which depend critically on good dielectric properties such as capacitive biosensor.

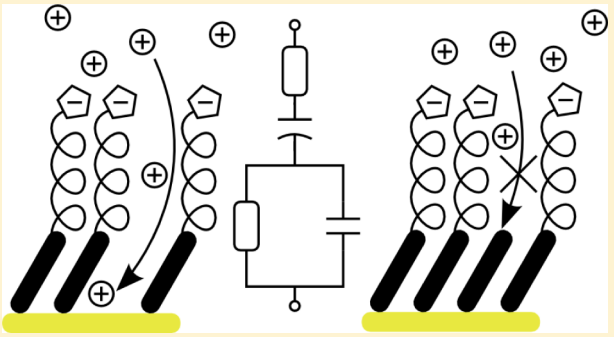

INTRODUCTION

Self-assembled monolayers (SAMs) are a versatile means for modifying the physical and chemical properties of surfaces,[1,2] including their hydrophobicity, biocompatibility,[2] antifouling properties,[3−5] and ability to bind molecules covalently.[4,6,7] They have been employed to modify a variety of surfaces including silicon oxide,[8] gold,[1,9] and other metals.[10,11] The exploitation of thiol-gold binding chemistry, and particularly in conjunction with molecules comprising alkane chains, provides an optimal combination of straightforward SAM preparation on gold surfaces, structural order, and versatility of modification of the functional group.[1,10]

SAMs are commonly used in electronic biosensors both to provide the chemical functionality to attach the receptor molecules[4] to the sensor surface required for the biological detection,[12] as well as serving as an antifouling layer to reduce unwanted, nonspecific binding of material such as protein molecules to the device surface.[3,13] SAMs of oligo- and poly-ethylene glycol chains (OEG, PEG) have been used extensively to reduce nonspecific protein absorption[2,3] and improve biocompatibility[4] on solid surfaces,[11,13] with OEG-terminated alkyl thiols often the preferred choice of SAM molecules on gold electrodes.[4,6,11,13] OEG-terminated alkyl thiols have been reported to form a SAM in which the alkane chains are tilted at a 30° angle with respect to the surface normal, with the terminal ethylene glycol groups forming either a liquid-like amorphous phase or a semicrystalline layer consisting of OEG molecules perpendicular to the surface.[11]

Carboxy groups are widely used to facilitate the specific attachment of capture molecules such as antibodies in biosensors. However, COOH-terminated OEG groups are bulky compared to the alkyl chains and hence sterically hinder the formation of a densely packed, well-ordered SAM,[11,13,14] leading to the presence of defects such as pinholes, and lower than expected SAM thickness.[11,13] In applications such as capacitance biosensors, where the receptor molecules are usually covalently bound to the functional group of the SAM, a well-ordered, highly packed SAM with low leakage and a high dielectric constant is required; the binding of the ligand to the receptor molecules changes the capacitance associated with the Stern layer, which forms the basis of the sensor.[15] However, the capacitance originating from the Stern layer can only be interrogated indirectly as a part of a series of capacitors that includes the capacitance of the SAM itself. Since the smallest capacitance in the series dominates the measurement, binding of ligands can only be detected if the SAM capacitance is

Received: October 14, 2013
Revised: December 20, 2013
Published: January 21, 2014

   dx.doi.org/10.1021/la403983b | *Langmuir* 2014, 30, 1321−1326

sufficiently high, and the presence of defects and pinholes in the monolayer is minimized.[15]

It has been suggested that small molecules can be added as spacers into the SAM among the OEG molecules to reduce steric hindrance caused by the bulky functional group.[3,6] Indeed it has been reported that OEG-terminated SAMs retain their antifouling properties even when diluted by up to 40% by alkanethiols.[16]

Here, we investigate the quality and dielectric properties of a range of OEG terminated SAMs with varying amounts of alkane thiol spacers, with the aim to reduce the number of defects in the SAMs and therefore enhance their dielectric properties for use in electrochemical biosensors. Owing to their excellent antifouling properties and the extensive use of OEG-alkanethiols for biosensing applications, a monolayer formed by carboxy-terminated (EG)-alkane chains was chosen for this study. The monolayer was characterized by electrochemistry, X-ray photoelectron spectroscopy (XPS), ellipsometry and contact angle measurements. The presence of defects in OEG SAMs, such as pinholes, is demonstrated by electrochemical impedance spectroscopy (EIS), where the phase of the impedance is found to increase considerably at low frequencies as expected for loosely packed monolayers.[17,18] Much improved dielectric properties are achieved by mixing the OEG terminated monolayer with different percentages of mercapto-undecanol (MUD) molecules.

MATERIALS AND METHODS

Materials. Acetone, absolute ethanol, methanol, Decon 90, platinum wire and silver/silver-chloride reference electrode (662-1795) were purchased from VWR International Ltd. (UK). 11-Mercapto-1-undecanol (MUD), glacial acetic acid, HCl, ethanol 200 proof, sodium phosphate monobasic monohydrate and sodium phosphate dibasic were sourced from Sigma-Aldrich Co (USA); (1-mercapto-11-undecyl)esa-ethylenglycol (OEG) and EPOTEK 353-ND were purchased from ProChimia Surfaces Sp.z o.o. (Poland) and Epoxy Technology Inc. (USA), respectively.

Monolayer Formation. MUD and OEG were dissolved in ethanol 200 containing 5% acetic acid at 0.5 mM. Different ratios of these solutions were mixed to yield solutions with final molar fractions of 0.05%, 0.1%, 0.5%, 1%, and 5% of MUD in OEG. At the same time 100% MUD and 100% OEG SAM solutions were prepared. The structure of both molecules is shown in Figure 1.

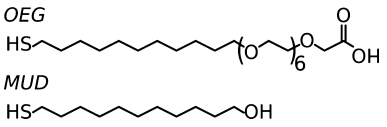

Figure 1. Skeletal model of the SAM molecules used for the formation of mixed monolayers in this study.

Template stripped gold samples were prepared as follows: SiO_2 capped Si wafers, used as templates, were cleaned by sonication in acetone, methanol, Decon 90 (1:20) and deionized (DI) water (Millipore, 18.2 MΩ) for 5 min each. Subsequently a gold layer, 120 nm thick, was directly deposited on the bare wafers by electron-beam evaporation at a base pressure of 10^{-7} mbar. Microscope slides were then cut to appropriate size and glued on the gold-coated wafers with a two-component epoxy glue, EPOTEK 353-ND. The glue was then cured for 2 min on a hot plate at 180 °C. The samples where thus kept at room temperature until used. Immediately before immersion in the SAM solutions, the glass slides were separated from the Si/SiO_2 wafer such that the gold was stripped from the template. The template stripped gold samples were then immediately transferred to the SAM solutions and incubated for 40 h. This method allows to keep the gold surface sealed by the template until use.

Different samples were prepared for electrochemical and contact angle measurements, while XPS and ellipsometry were carried out on the same samples.

Before measuring, each sample was rinsed with absolute ethanol, sonicated for 2 min in 0.2% HCl spiked ethanol, then rinsed and sonicated for 2 min in DI water. The samples were dried under a stream of dry N_2 and measured.

Electrochemical Impedance Spectroscopy. Electrochemistry measurements were performed using a three electrode configuration. A silver/silver-chloride electrode was used as the reference electrode, and a platinum wire as the counter electrode. The working electrode area (6.3 mm^2) was defined by rubber O-rings. The measurements were performed using a VSP potentiostat, Bio-Logic SAS (France), equipped with a low current option and acquisition software Ec-Lab.

Electrochemical impedance spectroscopy (EIS) was carried out in 100 mM sodium phosphate buffer at pH 7.2, after 20 min of preincubation in the same buffer. Impedance spectra over a frequency range from 50 mHz to 100 kHz were acquired by applying a sinusoidal signal of ±10 mV against open circuit voltage. Each measurement comprises three frequency scans, and three measurements were taken per sample at intervals of 20 min.

The impedance spectra were analyzed by fitting appropriate equivalent circuit models to the measured data (ProFit QuantumSoft, Switzerland).

Contact Angle Measurements. Contact angle measurements of static, advancing and receding water droplets were carried out for all monolayers. Multiple samples were prepared for each SAM, and four to six measurements were carried out per sample. Images were recorded digitally by means of a CCD camera and analyzed with ImageJ 1.46 software (National Institutes of Health, USA) equipped with the drop analysis plug-in.

The static angle was recorded by dispensing a droplet of DI water of about 1.5 μL volume from a square cut needle to the surface. The advancing angle was measured by reintroducing the needle in the center of the droplet and adding water until the contact line advances, while the receding angle was measured by retracting the water droplet until the contact line recedes.

Ellipsometry. The thickness of the SAM for each sample was estimated by means of null ellipsometry, using a Jobin-Yvon UVISEL instrument, and by using a clean template stripped gold sample as the reference surface. The measurements of the amplitude ratio, Ψ, and phase shift, Δ, were taken at an incident angle of 70°. The spectra were then fitted using DeltaPsi2, assuming a simple three-layer system. The SAM was modeled as a transparent thin film using a Cauchy dispersive model. The incident angle of the light was treated as a free parameter to allow for small deviations in the tilting angle caused by the way the template stripped gold samples were fabricated.

X-ray Photoelectron Spectroscopy. XPS spectra were obtained using a Thermo Electron Co ESCA Lab 250 system in ultra high vacuum. The chamber pressure was maintained lower than 10^{-9} mbar during data acquisition. Two sets of samples were irradiated by a monochromatic Al Kα X-ray beam (1486.7 eV) with a diameter of about 0.5 mm in two different regions. Survey and detailed scans were obtained in Large Area XL magnetic lens mode with a pass energy of 150 and 20 eV, respectively. The spectra were obtained with an electron take off angle of 90°.

Spectra were analyzed with the CasaXPS software, and all spectra were corrected by shifting the C 1s peak to 285.0 eV to compensate for residual charge on the surface. We note that the binding energies (BE) of uncorrected C 1s peaks were between 284.95 and 285.13 eV, except for one of the spots on the MUD:OEG 0.1% sample (BE of 285.49 eV).

For quantitative analysis of the XPS spectra, a 70−30% Gaussian−Lorentzian peak shape was used. The background was removed using a Shirley function for both Au 4f and C 1s peaks, while a linear function was used for the S 2p and O 1s.

dx.doi.org/10.1021/la403983b | Langmuir 2014, 30, 1321−1326

RESULTS AND DISCUSSION

EIS is a very sensitive tool for the investigation of the dielectric properties of SAMs and can reveal valuable information on the presence of defects such as pin holes. A range of mixed SAMs with MUD:OEG ratios of 0.05% to 5% as well as 100% MUD and OEG were investigated and the corresponding EIS measurements are shown in Figure 2.

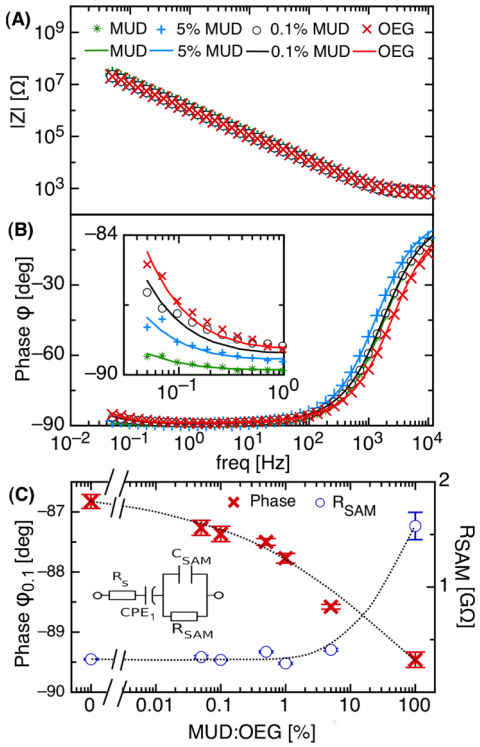

Figure 2. Typical (A) magnitude, |Z|, and (B) phase, φ, of the impedance of the SAMs as a function of frequency measured by EIS and corresponding fits (lines) for MUD (*), OEG (×) and the mixed SAMs: 0.1% (○) and 5% (+) MUD in OEG. The inset shows the detailed view at low frequencies. (C) phase of the impedance at 0.1 Hz, $\varphi_{0.1}$ (×), and SAM resistance, R_{SAM} (○), obtained from the fit to the impedance with the equivalent circuit shown in the inset, both plotted against the molar fraction of MUD to OEG in the solution used for the SAM formation. Standard deviation of the fitted parameter for R_{SAM} and between different scans for the phase, are shown as error bars. The dotted lines offer a guide to the eye.

For frequencies below about 1 Hz, an increase in phase of the impedance with decreasing concentrations of MUD in the monolayer solution was observed. Such a phase increase is characteristic for a rise in non-Faradaic charge transport through the SAM, e.g., caused by increasing numbers of defects or pinholes. In order to analyze these results, equivalent circuit models were employed to fit the impedance spectra.

Several equivalent circuit models have been proposed to approximate the electrochemical impedance of SAM-modified working electrodes. They generally comprise a network of four types of circuit elements: resistors (R), capacitors (C), as well as nonphysical elements such as constant-phase elements (CPE) or Warburg elements (W). The impedance of these elements is defined as follows:

$$Z_R = R;$$

$$Z_C = 1/(j\omega C);$$

$$Z_{CPE} = 1/((j\omega)^{\alpha} Q), \quad \alpha \leq 1;$$

$$Z_W = 1/((j\omega)^{1/2} W)$$

The Warburg element and the capacitor are special cases of the CPE where α is equal to 0.5 or 1, respectively.

Thin, defect-free SAMs are often approximated by an ideal Helmholtz capacitor,[15,19] and therefore the impedance of the system can be modeled by a capacitor in series with a resistor representing the solution resistance. The phase of the impedance of this circuit approaches −90° at low frequencies, which is clearly not the case here.

A more realistic equivalent circuit model can be derived from the analysis of the impedance spectra.[19] The phase spectra of the OEG and the mixed monolayers (Figure 2B) show a minimum of −89° at about 1 Hz, and the phase increases for lower frequencies. Therefore, we conclude that the equivalent circuit should present two time constants and that the capacitive components are nonideal, i.e., they should be represented by constant phase elements. Moreover, we note that the increase in phase is not due to a faradaic current as the measurements were performed in absence of redox probes. Hence, the circuit shown in Figure 3 was used to model the impedance data.

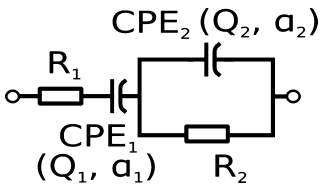

Figure 3. Equivalent circuit employed to fit the electrode solution interface.

The impedance spectra of all SAMs were fitted using this equivalent circuit, and initially all parameters were left free to vary. The parameter α_2 of the constant phase element CPE_2 consistently reached the limit of 1 for all samples, and hence the CPE was replaced by an ideal capacitor. Furthermore, since R_1 is generally associated with the solution resistance[19,20] (R_s) which is governed by the buffer strength and the geometry of the cell, it was fixed for all samples to 647 Ω which corresponds to the average of R_1 of all investigated SAMs.

The remaining circuit elements can be associated with the solution/electrode interface. We note that R_2 and CPE_2 constitute a leaky capacitor, often used for modeling defects in the SAM,[17] therefore we will refer to these elements as R_{SAM} and C_{SAM} (Figure 2C, inset). The quality of the fits to the data depends only weakly on the value of α_1 within a small range, and therefore α_1 was fixed to the average of all fitted α_1 (α_1 = 0.82) to simplify data interpretation.

Both R_{SAM} and the phase of the impedance at 0.1 Hz ($\varphi_{0.1}$) are plotted in Figure 2C as a function of percentage of MUD in the SAM solution used to generate the monolayers.

We note that both a smaller SAM resistance as well as a higher than −90° phase for frequencies smaller than 1 Hz can be interpreted as an increased number of pin-holes in the SAM.[18] The increase of R_{SAM} with the MUD molar fraction in

dx.doi.org/10.1021/la403983b | Langmuir 2014, 30, 1321−1326

solution indicates an improvement in SAM integrity, probably due to a better packing of the SAM molecules (Figure 2).[15,19]

A perfectly packed monolayer is expected to behave like an ideal capacitor,[15,19] and at low frequencies the phase is expected to be equal to −90° and the SAM resistance infinite. For the MUD monolayer, a phase lower than −89.5° was found at frequencies below 10 Hz, and the fitted R_{SAM} for MUD is equal to 1.6 ± 0.1 GΩ, indicating that MUD forms a well packed monolayer with a negligible amount of pinholes, as expected. The opposite is found for the 100% OEG SAM, where the phase at 0.1 Hz and R_{SAM} are equal to −86.8° ± 0.1° and 315 ± 6 MΩ, respectively. This is consistent with the hypothesis that monolayers formed from 100% OEG are considerably less well packed than MUD SAMs.

It has been reported that the steric hindrance caused by the ethylene glycol (EG) chains should not interfere significantly with the formation of a well-packed monolayer[11] because the cross section of the coiled EG groups is compatible with the alkane chain spacing for packed SAMs.[11] However, the carboxylic acid present in OEG molecules might lead to a less well packed and therefore less insulating monolayer, as it was observed in this study. Nevertheless, by adding even a small amount of MUD, i.e., 0.1% or more, to the SAM solution, the SAM resistance increases noticeably (Figure 2C) and the phase decreases (Figure 2C). This suggests that the small number of MUD embedded into the mixed SAM can relax the stress between the OEG molecules and therefore lead to better packing, which in turn results in much improved dielectric properties.

The ratio of molecules absorbed on the surface is not necessarily the same as the molar ratio in solution, as the absorption depends on the reaction kinetics of each molecule and the solvent.[3,5] However, it is possible to establish experimentally which conditions of the SAM formation (such as stoichiometry of the solution, solvent and incubation time) will give the desired properties of the SAM on the surface and therefore reliably form the required monolayer.[3,5] Moreover, depending on the intermolecular interactions, the mixed SAM will either be homogeneous or will show clusters of molecules of the same type.[5]

As a preliminary characterization of the different monolayers, the wetting properties of the mixed SAMs have been studied by means of water contact angle. The results for static apparent contact angle (θ_s) are shown in Figure 4. The 100% MUD monolayer showed a very low static contact angle (θ_s = 13° ± 3°) as expected for a well ordered hydrophilic layer. The advancing (θ_a) and receding (θ_r) apparent contact angles were found to be 19° ± 1 and 10° ± 1°, respectively. In contrast, the OEG monolayer showed a static contact angle of 37° ± 1°, θ_α = 38° ± 2° and θ_r = 26° ± 2°, which is in good agreement with values reported in the literature for very similar SAMs (θ_α = 38° and θ_r = 25°).[9] Interestingly, the mixed SAMs all showed static contact angles of around 30°, independent of the MUD concentration in the SAM solution.

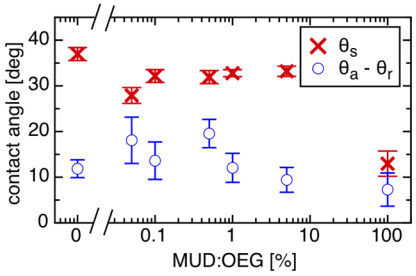

Figure 4. Static water contact angle, θ_s(×), and hysteresis, $\theta_a - \theta_r$ (○), for all monolayers plotted against the molar fraction of MUD in OEG.

The hysteresis, defined as the difference between the advancing (θ_a) and receding (θ_r) apparent contact angles, $\theta_h = \theta_a - \theta_r$, is an indication of both roughness and chemical homogeneity and thus the distribution of MUD and OEG on the surface.[21,22] The hysteresis is relatively small for the MUD SAM (θ_h = 9° ± 3°), and it increases for mixed MUD:OEG SAMs reaching saturation for concentration of MUD smaller than 1% (e.g., θ_h = 22° ± 1° for 0.5% MUD). These results can be interpreted in the light of the hypothesis that the mixed SAMs form islands or clusters of OEG and mixed SAMs, and the raised OEG islands behave like geometrical defects. The presence of islands increases the hysteresis but for increasing MUD percentage the density of OEG islands decreases, thus the decreasing hysteresis.[22]

The quality of a SAM in terms of packing density is reflected in its thickness. The molecules in alkane-thiol-based SAMs are generally tilted away from the surface normal by around 30°. A reduction in packing usually results in a reduction of this tilt angle, and hence in an increase of the monolayer thickness.

The theoretical thickness of the OEG SAM is equal to 34.9 Å, taking into account the C−S bond, the 11-carbon alkyl chain tilted at 30°, the carboxylic acid and assuming a helical conformation of the EG groups with a length of 2.78 Å per EG.[11] The thickness of the MUD SAM, using the same assumption, is estimated to be 14.4 Å (Table 1).

Table 1. Average SAM Thickness Estimated by Ellipsometry, with the Fitting Error

monolayer	thickness [Å]	error [Å]
100% OEG	35.5	2.0
0.05% MUD	36.8	0.9
0.1% MUD	34.9	1.5
1% MUD	34.8	1.4
5% MUD	31.9	1.1
100% MUD	14.5	0.8

We estimated the thicknesses of all SAMs by ellipsometry, and the results are given in Table 1. The measurements for the OEG and MUD SAM are in excellent agreement with the expected values: 14.5 ± 0.8 Å for MUD, and 36 ± 2 Å for OEG, suggesting that the monolayers have the alkyl chains indeed tilted at a 30° angle and the EG groups are in a helical conformation. We note that only for MUD percentages bigger than 1% a significant decrease in the average thickness is observed, while all other SAMs show a thickness similar to the OEG monolayer.

The chemical composition of the assembled monolayers was studied by XPS, and the results are summarized in Table 2. First, a survey scan was carried out, and only peaks corresponding to Au, C, O and S were detected, with no additional peaks observed. Detailed scans were then recorded for the Au 4f, C 1s, O 1s and S 2p peaks, and typical spectra are shown in the supplementary data (Figure S1, Supporting Information). From these, the relative elemental composition of the different SAMs was estimated taking into account the relative sensitivity factor of the instrument automatically

dx.doi.org/10.1021/la403983b | Langmuir 2014, 30, 1321−1326

Table 2. Summary of Quantitative Analysis of XPS Spectra

Theoretical Values						
monolayer	C 1s %	O 1s %	S 2p %	C:S	C:O	O:S
OEG	71.4	25.7	2.9	25	3	9
MUD	84.6	7.7	7.7	11	11	1
Measured Values						
monolayer	C 1s %	O 1s %	S 2p %	C:S	C:O	O:S
100% OEG	75.9	22.2	2.7	33.6	3.4	9.8
0.05% MUD	77.0	20.8	2.2	35.0	3.7	9.5
0.1% MUD	71.3	26.1	2.6	27.7	2.7	10.1
0.5% MUD	77.7	20.5	1.8	42.5	3.8	11.2
1% MUD	76.2	21.4	2.5	30.7	3.6	8.6
5% MUD	77.2	20.2	2.6	29.5	3.8	7.7
100% MUD	89.2	6.9	3.9	22.7	13.0	1.8

(XPSCasa). The results, together with the theoretical values, are reported in Table 2.

As expected, the S 2p signal is consistently lower than the theoretically expected value, as the signal is suppressed by the presence of the monolayer, thus leading to inflated element-to-sulfur ratios.

Considering that the C 1s peak has a non-negligible component corresponding to the C═O bond (BE = 289.3 eV) only for the SAMs which contain OEG (i.e., 100% OEG and mixed SAMs) but not for 100% MUD, the C═O component can be used to estimate the percentage of OEG molecules on the surface (for further details, see the Supporting Information). The theoretical value of COOH:S ratio for the 100% OEG SAM is 1, but, as previously discussed, the S 2p peak is attenuated so the experimentally determined value is likely to be higher, and it is in fact found to be equal to 1.4 ± 0.3. In Figure 5 the COOH:S ratio is plotted for all SAMs

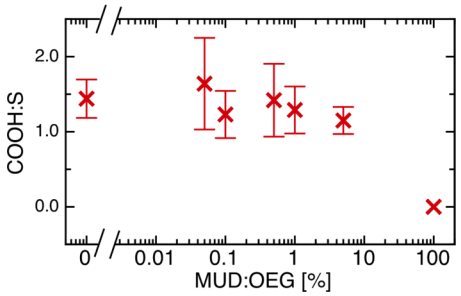

Figure 5. COOH:S ratio calculated from XPS data; error bars represent the standard deviation.

against the percentage of MUD in the SAM formation solution. We note that the COOH:S ratio shows a very similar behavior as the monolayer thickness, showing little difference between the 100% OEG SAM and the mixed monolayers with MUD concentrations up to 0.1%. For higher MUD concentrations, both the COOH:S ratio and the monolayer thickness decrease toward zero. We speculate that these quantities represent a good measure for the surface ratio of MUD to OEG molecules.

To compare the data obtained by EIS, ellipsometry, and XPS, we normalized all data by fixing the value for 100% MUD of each data set to zero and the one for 100% OEG to one. The resulting data, phase of the impedance at 0.1 Hz, the conductivity of the SAM ($G_{SAM} = 1/R_{SAM}$), the monolayer thickness, and the COOH:S ratio, are shown in Figure 6.

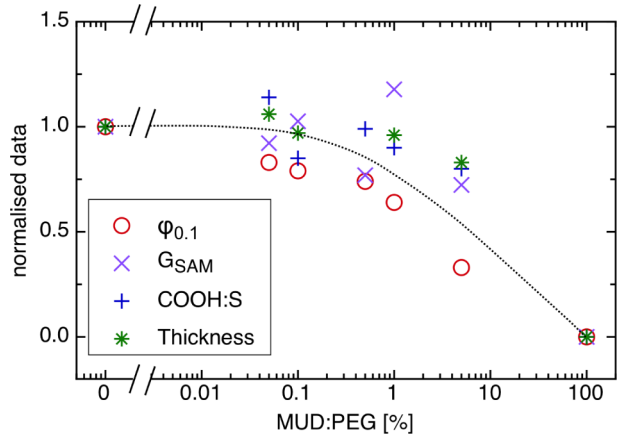

Figure 6. Normalized phase at 0.1 Hz, $\varphi_{0.1}$ (○), SAM conductivity, G_{SAM} (×), carboxylic acid to sulfur ratio, COOH:S (+), and SAM thickness, (*). The solid line offers a guide to the eye.

We note that all data follow the same nonlinear behavior, with little difference between the 100% OEG SAM and the mixed SAMs with small MUD concentration (MUD < 0.5%) followed by a rapid decrease of the quantity toward 100% MUD.

CONCLUSIONS

Electrochemical impedance spectroscopy was used to characterize the dielectric properties of OEG and mixed MUD:OEG SAMs. An equivalent circuit model has been proposed to model the presence of defects in the monolayers. XPS, ellipsometry and contact angle have been used to characterize the composition of the monolayers.

This study shows that even a small amount of MUD in the mixed MUD:OEG SAMs leads to considerably improved dielectric properties, as seen by the considerable decrease of the phase of the impedance at low frequencies as well as a significant increase in the resistivity of the SAM.

Systems which rely on SAMs with good dielectric properties such as electrochemical biosensors, and in particular capacitive sensors, will benefit significantly from such mixed MUD:OEG SAMs.

ASSOCIATED CONTENT

Supporting Information

XPS survey scans and detailed scans of Au 4f, C 1s, O 1s, and S 2p are shown in Figure S1 for both 100% MUD and 100% OEG monolayers. This information is available free of charge via the Internet at http://pubs.acs.org.

AUTHOR INFORMATION

Corresponding Author

*E-mail: c.walti@leeds.ac.uk.

Notes

The authors declare no competing financial interest.

ACKNOWLEDGMENTS

This work was in part funded through BBSRC, Abbott Laboratories, and WELMEC, a Centre of Excellence in Medical Engineering funded by the Wellcome Trust and EPSRC, under grant number WT 088908/Z/09/Z. We also acknowledge support of the Royal Society and Wolfson Foundation.

REFERENCES

(1) Bain, C.; Troughton, E.; Tao, Y.; Evall, J.; Whitesides, G.; Nuzzo, R. Formation of monolayer films by the spontaneous assembly of organic thiols from solution onto gold. *J. Am. Chem. Soc.* **1989**, *111*, 321−335.

(2) Yang, Z.; Galloway, J.; Yu, H. Protein interactions with poly(ethylene glycol) self-assembled monolayers on glass substrates: Diffusion and adsorption. *Langmuir* **1999**, *15*, 8405−8411.

(3) Chapman, R.; Ostuni, E.; Yan, L.; Whitesides, G. Preparation of mixed self-assembled monolayers (SAMs) that resist adsorption of proteins using the reaction of amines with a SAM that presents interchain carboxylic anhydride groups. *Langmuir* **2000**, *16*, 6927−6936.

(4) Herrwerth, S.; Rosendahl, T.; Feng, C.; Fick, J.; Eck, W.; Himmelhaus, M.; Dahint, R.; Grunze, M. Covalent coupling of antibodies to self-assembled monolayers of carboxy-functionalized poly(ethylene glycol): Protein resistance and specific binding of biomolecules. *Langmuir* **2003**, *19*, 1880−1887.

(5) Love, J.; Estroff, L.; Kriebel, J.; Nuzzo, R. Self-assembled monolayers of thiolates on metals as a form of nanotechnology. *Chem. Rev.* **2005**, *105*, 1103−1169.

(6) Anderson, A.; Dattelbaum, A.; Montaño, G.; Price, D.; Schmidt, J.; Martinez, J.; Grace, W.; Grace, K.; Swanson, B. Functional PEG-modified thin films for biological detection. *Langmuir* **2008**, *24*, 2240−2247.

(7) Samanta, D.; Sarkar, A. Immobilization of bio-macromolecules on self-assembled monolayers: Methods and sensor applications. *Chem. Soc. Rev.* **2011**, *40*, 2567−2592.

(8) Bigelow, W.; Pickett, D.; Zisman, W. Oleophobic monolayers: I. Films adsorbed from solution in non-polar liquids. *J. Colloid Sci.* **1946**, *1*, 513−538.

(9) Pale-Grosdemange, C.; Simon, E.; Prime, K.; Whitesides, G. Formation of self-assembled monolayers by chemisorption of derivatives of oligo(ethylene glycol) of structure HS-$(CH_2)_{11}(OCH_2CH_2)_mOH$ on gold. *J. Am. Chem. Soc.* **1991**, *113*, 12−20.

(10) Ulman, A. Formation and structure of self-assembled monolayers. *Chem. Rev.* **1996**, *96*, 1533−1554.

(11) Harder, P.; Grunze, M.; Dahint, R.; Whitesides, G.; Laibinis, P. Molecular conformation in oligo(ethylene glycol)-terminated self-assembled monolayers on gold and silver surfaces determines their ability to resist protein adsorption. *J. Phys. Chem. B* **1998**, *102*, 426−436.

(12) Katz, E.; Willner, I. Amperometric amplification of antigen-antibody association at monolayer interfaces: Design of immunosensor electrodes. *J. Electroanal. Chem.* **1996**, *418*, 67−72.

(13) Wang, R.; Kreuzer, H.; Grunze, M. Molecular conformation and solvation of oligo(ethylene glycol)-terminated self-assembled monolayers and their resistance to protein adsorption. *J. Phys. Chem. B* **1997**, *101*, 9767−9773.

(14) Wang, H.; Chen, S.; Li, L.; Jiang, S. Improved method for the preparation of carboxylic acid and amine terminated self-assembled monolayers of alkanethiolates. *Langmuir* **2005**, *21*, 2633−2636.

(15) Berggren, C.; Bjarnason, B.; Johansson, G. Capacitive biosensors. *Electroanalysis* **2001**, *13*, 173−180.

(16) Prime, K.; Whitesides, G. Adsorption of proteins onto surfaces containing end-attached oligo(ethylene oxide): a model system using self-assembled monolayers. *J. Am. Chem. Soc.* **1993**, *115*, 10714−10721.

(17) Boubour, E.; Lennox, R. Stability of omega-functionalized self-assembled monolayers as a function of applied potential. *Langmuir* **2000**, *16*, 7464−7470.

(18) Boubour, E.; Lennox, R. Potential-induced defects in *n*-alkanethiol self-assembled monolayers monitored by impedance spectroscopy. *J. Phys. Chem. B* **2000**, *104*, 9004−9010.

(19) Boubour, E.; Lennox, R. Insulating properties of self-assembled monolayers monitored by impedance spectroscopy. *Langmuir* **2000**, *16*, 4222−4228.

(20) Randles, J. E. B. Kinetics of rapid electrode reactions. *Discuss. Faraday Soc.* **1947**, *1*, 11.

(21) Decker, E.; Frank, B.; Suo, Y.; Garoff, S. Physics of contact angle measurement. *Colloids Surf., A* **1999**, *156*, 177−189.

(22) Reyssat, M.; Quéré, D. Contact angle hysteresis generated by strong dilute defects. *J. Am. Chem. B* **2009**, *113*, 3906−3909.